Potential impact of subsonic and supersonic aircraft exhaust on water vapor in the lower stratosphere assessed via a trajectory model

Gary A. Morris
Department of Physics and Astronomy, Rice University, Houston, Texas, USA

Joan E. Rosenfield
GEST Center, University of Maryland Baltimore County, Baltimore, Maryland, USA

Mark R. Schoeberl and Charles H. Jackman
Laboratory for Atmospheres, NASA Goddard Space Flight Center, Greenbelt, Maryland, USA

Received 4 June 2002; revised 15 July 2002; accepted 15 July 2002; published 6 February 2003.

[1] We employ a trajectory model to assess the impact on the stratosphere of water vapor present in the exhaust of subsonic and a proposed fleet of supersonic aircraft. Air parcels into which water vapor from aircraft exhaust has been injected are run through a 6-year simulation in the trajectory model using meteorological data from the UKMO analyses with emissions dictated by the standard 2015 emissions scenario. For the subsonic aircraft, our results suggest maximum enhancements of ~150 ppbv just above the Northern Hemisphere tropopause and of much less than 50 ppbv in most other regions. Inserting the perturbed water vapor profiles into a radiative transfer model, but not considering the impact of additional cirrus formation resulting from emissions by subsonic aircraft, we find that the impact of subsonic water vapor emissions on the radiative balance is negligible. For the supersonic case, our results show maximum enhancements of ~1.5 ppmv in the tropical stratosphere near 20 km. Much of the remaining stratosphere between 12 and 25 km sees enhancements of greater than 0.1 ppmv, although enhancements above 35 km are generally less than 50 ppbv, in contrast to previous 2-D and 3-D model studies. Radiative calculations based upon these projected water vapor perturbations indicate they may cause a nonnegligible impact on tropical temperature profiles. Since our trajectory model includes no chemistry and our radiative calculations use the most extreme water vapor perturbations, our results should be viewed as upper limits on the potential impacts. *INDEX TERMS:* 0341 Atmospheric Composition and Structure: Middle atmosphere—constituent transport and chemistry (3334); 1610 Global Change: Atmosphere (0315, 0325); 3334 Meteorology and Atmospheric Dynamics: Middle atmosphere dynamics (0341, 0342); 3337 Meteorology and Atmospheric Dynamics: Numerical modeling and data assimilation; *KEYWORDS:* stratospheric water vapor, trajectory modeling, temperature perturbations, subsonic aircraft emissions, supersonic aircraft emissions

Citation: Morris, G. A., J. E. Rosenfield, M. R. Schoeberl, and C. H. Jackman, Potential impact of subsonic and supersonic aircraft exhaust on water vapor in the lower stratosphere assessed via a trajectory model, *J. Geophys. Res.*, *108*(D3), 4103, doi:10.1029/2002JD002614, 2003.

1. Introduction

[2] Water vapor is an important trace constituent in the atmosphere due to its radiative, chemical, and when condensed, aerosol properties. Aircraft exhaust is responsible for injecting ~1.24 kg of water vapor for every kilogram of fuel burned. With emissions based on an updated version of work by *Baughcum et al.* [1998], aircraft inject ~80 Mtons of water vapor into the stratosphere each year in our model. Due to the extent and frequency of commercial aviation and the importance of water vapor in climate, numerous previous studies have attempted to assess the impact of water vapor perturbations due to aircraft exhaust on the troposphere and lower stratosphere. These previous efforts have employed general circulation models (GCMs) [e.g., *Ponater et al.*, 1996; *Marquart et al.*, 2001], 2-D and 3-D models [e.g., *Weaver et al.*, 1996; *Danilin et al.*, 1998; *Kawa et al.*, 1999; *Nevison et al.*, 1999; *Rodgers et al.*, 2000; *Kinnison et al.*, 2001], and radiative transfer calculations [e.g., *Fortuin et al.*, 1995]. Many of the previous modeling results are summarized by *Brasseur et al.* [1998], *Kawa et al.* [1999], and *Penner et al.* [1999].

[3] Increases in stratospheric water vapor can have several important consequences, both direct and indirect. Radiative feedback from increased levels of water vapor may lead to changes in tropopause temperature and/or height. The fre-

0148-0227/03/2002JD002614$09.00

quency of the formation of contrails, cirrus, or subvisible cirrus clouds may increase, further impacting the radiative balance [e.g. *Rosenfield*, 1998]. The frequency and persistence of polar stratospheric clouds (PSC) may increase, leading to more substantial springtime ozone loss in the polar regions [*Kawa et al.*, 1999, chapter 4]. Changes in the temperature of the tropopause can lead to changes in the flux of water vapor into the stratosphere [*Kawa et al.*, 1999, chapter 2].

[4] Chemically, an increase in water vapor can have an impact on ozone in the lower stratosphere through the HO_x cycle, which is responsible for 30–50% of the ozone losses in the lower stratosphere [*Wennberg et al.*, 1994]. In their 2-D model study, *Nevison et al.* [1999] imposed a doubling of water vapor at the tropopause from 4 ppmv to 8 ppmv that resulted in 0–6% losses in ozone between 10 and 30 km altitude with halogens at 1996 levels. *Kawa et al.* [1999] conclude that in the aerosol free stratosphere, ozone perturbations are primarily driven by perturbations in HO_x from H_2O emissions from supersonic aircraft with emissions indices (EI) for NO_x species less than 10 g of NO_x per kilogram of fuel burned.

[5] Many of these potential consequences (radiative and chemical) of increased water vapor from aircraft exhaust have been investigated previously. Almost uniformly, these previous assesments have determined that the impact of the exhaust from the subsonic fleet of aircraft on the water vapor profile in the lower stratosphere is entirely negligible [*Danilin et al.*, 1998; *Ponater et al.*, 1996; *Rind et al.*, 1996]. Although the water vapor perturbations are small, such changes could still be important radiatively if they could lead to changes in the formation of contrails or cirrus clouds. Such clouds could have either a warming (winter) or cooling (summer) effect on the atmosphere near the tropopause [*Fortuin et al.*, 1995]. In order to have a significant impact on the global climate, however, *Ponater et al.* [1996] suggest that contrails need to cover about 5% of the sky, whereas satellite data suggest coverage of less than 2% [*Bakan et al.*, 1994]. Only when the perturbation reaches a significant fraction of the annual variability of the backgroundwater vapor can sufficient changes in the area of the sky covered by contrails be generated [*Ponater et al.*, 1996]. A recent modeling study by *Rind et al.* [2000] suggests that increases in cirrus cloud coverage of 1% over current levels in the 12–15 km altitude range along aircraft flight paths can lead to global temperature changes of ~0.4 C with the largest effects being observed in the upper troposphere. For a further discussion of the impact of cirrus clouds, see work by *Penner et al.* [1999] and *Brasseur et al.* [1998]. For the purposes of this study, however, we will ignore the possible formation of additional cirrus clouds.

[6] In this study we employ an entirely different approach to the problem of determining the lower stratospheric water vapor perturbation resulting from aircraft exhaust. We use the Goddard Trajectory Model [*Schoeberl and Sparling*, 1995] to passively advect water vapor in the lower stratosphere as a trace gas. Since our model includes no chemical conversion of water vapor to other hydrogen species, our results should be viewed as an upper limit on the potential water vapor perturbation due to emissions from subsonic and a proposed fleet of supersonic aircraft. When our simulation has attained an equilibrium water vapor perturbation, we use several of the largest water vapor perturbation profiles in a radiative transfer model [*Rosenfield et al.*, 1994] to obtain an estimate of the impact on temperatures.

[7] One of the main advantages of the trajectory approach is that the dynamic lifetime of the water vapor is controlled by the atmospheric transport prescribed by the wind fields and heating rates employed in the model. Unlike 2-D and 3-D models in which water vapor can be transported through diffusion processes, the trajectory model employs a Lagrangian transport scheme that traces an exact path for each individual air parcel. Removal of water vapor is controlled by dynamics and occurs when a parcel reaches a level more than 0.5 km below the local tropopause along its trajectory. This approach differs with previous studies in which lifetimes and removal processes were externally imposed (e.g., removal below 7 km altitude with a timescale of 5 days as given by *Danilin et al.* [1998]). Other studies have imposed lifetimes of 0.5 to 2.5 years [*Fortuin et al.*, 1995], but have had difficulty in determining how much water vapor can accumulate in the lower stratosphere from years of aircraft emissions. An estimate for the equilibrium cumulative level of the water vapor perturbation is a direct result from the trajectory approach.

[8] In the next section, we review the trajectory approach to this problem as previously applied by *Schoeberl et al.* [1998] and *Schoeberl and Morris* [2000]. We then discuss the results from the trajectory model and from our radiative transfer calculations for both the subsonic and supersonic emissions.

2. Methodology

[9] We follow the procedure outlined by *Schoeberl and Morris* [2000] with the difference being that for this study, we initialize parcels based on the water vapor associated with aircraft emissions rather than the nitrogen species. To review, we inject the parcels into the trajectory model [*Schoeberl and Sparling*, 1995] every 5 days for forward integration. The initialization scheme is based upon the predicted traffic for aircraft in 2015 and an updated version of emissions given by *Baughcum et al.* [1998]. For the subsonic aircraft, our exhaust scenario varies through the year in accordance with known seasonal variation in flight traffic. For the supersonic results, we use a projected fleet of 500 aircraft and emissions from Models and Measurements II [*Penner et al.*, 1999, chapter 9]. Unlike the subsonic emissions, supersonic emissions are assumed to be constant throughout the year for purposes of initializing our trajectory model. We convert the given emission rate from molecules per cubic centimeter per second to air parcels per unit volume per day. The location of initialized parcels includes a random component to simulate variability due to local weather events. As noted by *Schoeberl and Morris* [2000], although our initialization process results in a patchy distribution rather than the smoother and more continuous fields of the actual emissions, the results will be statistically the same.

[10] Figures 1a and 1b show the zonal mean, annual water vapor perturbation resulting from emissions of the subsonic and supersonic aircraft, respectively. (These figures can be compared to later figures showing the equilibrium distribution of the water vapor perturbation.) Overlaid on the emissions plots are the potential temperature isentropes

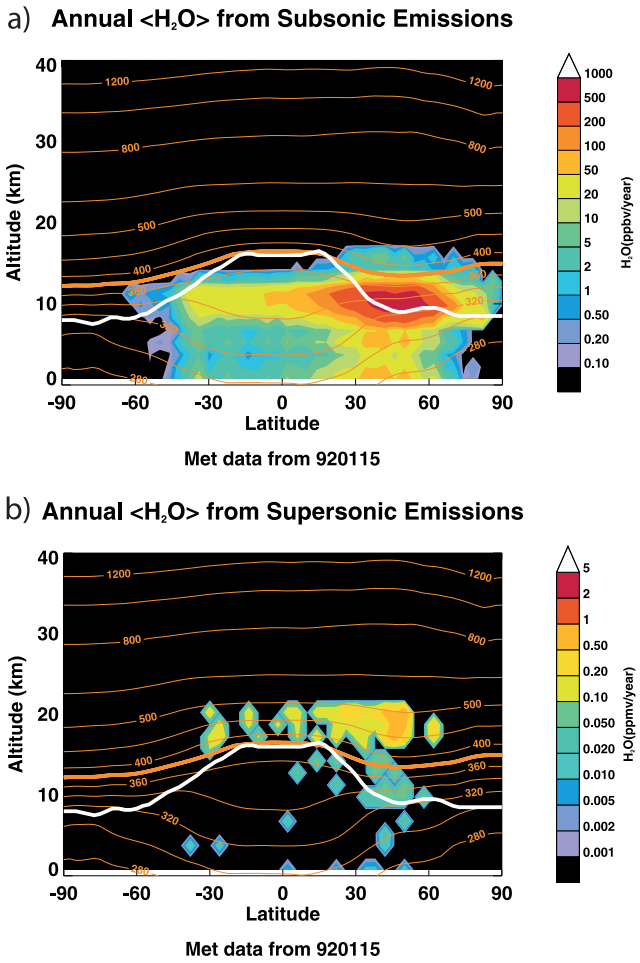

Figure 1. Annual zonal mean H_2O emission rates as a function of altitude for (a) subsonic and (b) supersonic aircraft in ppmv/year. The thick white line is the zonal mean tropopause for January 15, 1992. Thin orange lines show the potential temperature contours for the same day. The 380 K isentrope is represented by the thick orange line.

(thin orange lines), the 380 K potential temperature surface (thick orange line; conventionally considered the boundary between the middleworld and the overworld stratosphere), and the tropopause (thick white line) for January 15, 1992. Note that we define the tropopause as the lesser of the following two quantities: the height at which the minimum temperatures in the profile occurs and the height of the 3 potential vorticity unit (PVU) level. Clear from Figures 1a and 1b is the fact that the subsonic aircraft emissions are primarily generated in the Northern Hemisphere lower stratosphere near the tropopause, while the supersonic emissions are almost entirely above the tropopause in the Northern Hemisphere stratosphere. Except for a scaling factor, the emission data shown here for water vapor have the same morphology as those for NO_y given by *Schoeberl and Morris* [2000], as expected.

[11] After each 5 days of integration, the model removes those parcels that have been transported to 0.5 km or more below the local tropopause. Real temperature profiles often make finding the precise location of the tropopause difficult. The amount of exhaust entering the lower stratosphere, particularly in the subsonic aircraft emissions case, is quite sensitive to this definition [*Gettelman and Baughcum*, 1999]. The rapidity with which emissions near the tropopause return to the troposphere, however, tends to make our results somewhat insensitive to the definition of the tropopause.

[12] The trajectory model includes no chemical or photochemical reactions. As such, the number of water vapor molecules is strictly conserved along the calculated trajectories. The only loss mechanism for water vapor is transport to the troposphere. The model does not take into account the effect of background levels of water vapor or production of water vapor by any other mechanisms.

[13] The trajectory model employs diabatic calculations and winds from the United Kingdom Met Office (UKMO) stratospheric assimilation system [*Swinbank and O'Niell*, 1994] to transport the parcels. UKMO winds are produced once per day at noon Universal Time (UT) on a 2.5° latitude × 3.75° longitude grid. Heating rates for the diabatic calculations are derived from the UKMO data using the radiative transfer model of *Rosenfield et al.* [1994]. Air parcel trajectories are computed using a time step of one fiftieth of a day. At each time step in the model, winds and heating rates are interpolated in time and space to the location of each parcel before calculating the next spatial displacement along the trajectory. We note that *Schoeberl et al.* [1998] found that trace species lifetimes as calculated using long-duration trajectory runs show little to no dependence upon the meteorological wind field data set employed.

[14] Our simulation runs for 6 years using 4 years of meteorological data (1992–1995 inclusive): We recycle the meteorological data after 4 years; that is, year 5 has the same meteorology as year 1. At the end of this 6-year period, the annual mean number of parcels has effectively reached an equilibrium state, so we expect little change to occur in the mean behavior beyond year 6 of the simulation.

3. Results

3.1. Subsonic Emissions

[15] Figure 2a shows the trajectory results for the equilibrium zonal mean perturbation in June 1998 caused by the injection of water vapor from subsonic aircraft. Overlaid on the figure, as in Figure 1, are the potential temperature surfaces (orange lines) and the tropopause (thick white line). Figures 2a (subsonic) and 2b (supersonic) depict results from the month of June in order to facilitate comparison with the previously published water vapor perturbation results that also show the month of June [*Kawa et al.*, 1999; *Penner et al.*, 1999; *Kinnison et al.*, 2001]. We see that most of the stratosphere experiences little to no perturbation (less than 2 ppbv). The bulk of the water vapor perturbation occurs in the Northern Hemisphere (latitudes >30°N), lower stratosphere just above the tropopause, with peak values of <100 ppbv (note: higher peak values of ~150 ppbv are observed near 80°N in the corresponding plot for February 1998, not shown). Our subsonic water vapor perturbation distribution has a similar morphology to the subsonic NO_y perturbation distribution shown in Plate 3b of *Schoeberl and Morris* [2000], as we would expect. Our water vapor perturbations are consistent with, although on the low end of those given by *Fortuin et al.* [1995] of 76 to 380 ppbv, but our results are higher than those found by *Marquart et al.* [2001]. Since we

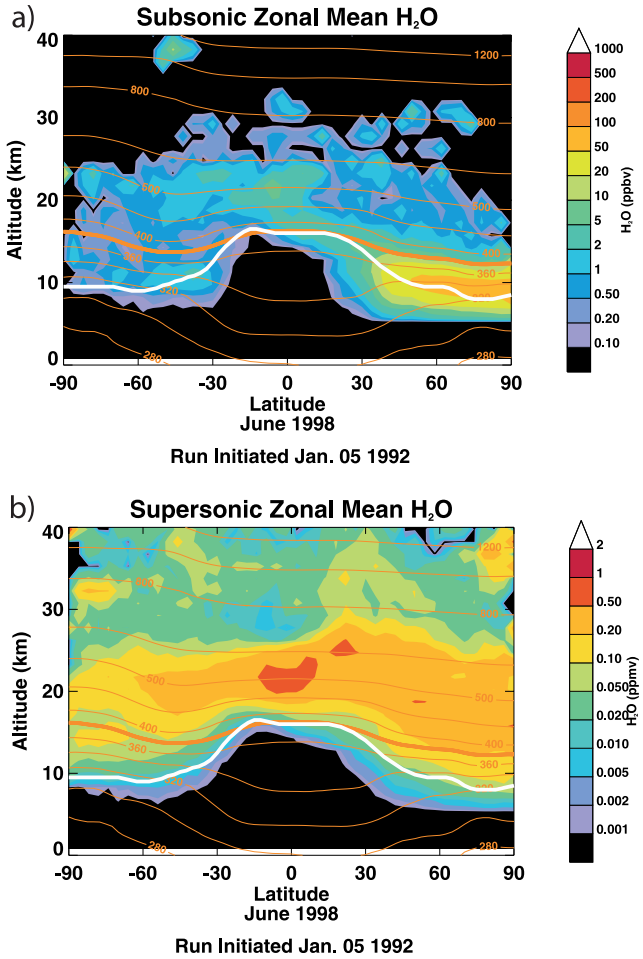

Figure 2. Zonal mean H_2O perturbation averaged over the month of June 1998 for the (a) subsonic and (b) supersonic aircraft emissions cases. Again, the thick white line is the zonal mean tropopause, this time for June 15, 1998. The thin orange lines are potential temperature contours for the same day. The 380 K isentrope is represented by the thick orange line.

include no mechanisms for the removal of water vapor other than descent through the tropopause, we are not surprised that our resulting water vapor perturbation may exceed those found in other studies. If the radiative impact of our water vapor perturbation profile is negligible, however, then we need not pursue a more realistic simulation of loss processes nor more detailed radiative calculations.

[16] The water vapor perturbation data vary with maximum values ranging from ~70 to ~150 ppbv and with a seasonal cycle that coincides well with the fraction of emissions that are deposited directly into the stratosphere as reported by *Gettelman* [1998] and *Gettelman and Baughcum* [1999]. To examine the radiative impact of the water vapor perturbations predicted by the trajectory model, we first calculate a monthly mean water vapor perturbation profile for each month in each year of our study. Then we calculate profiles of the associated standard deviations for each month in each year of our study. Next, we construct a new and extreme set of water vapor perturbation profiles by adding to each monthly mean profile twice the associated standard deviation profile for that month and year. Two of the largest resulting profiles in this new set of profiles occur in January 1997 at 54°N and in January 1996 at 82°N. These profiles are fed into the radiative transfer model of *Rosenfield et al.* [1994]. Radiatively determined temperatures are calculated by time integrating the radiative heating forward with a seasonal cycle. Tropospheric temperatures below 400 hPa are specified using a time-varying climatology. With this approach, we effectively compute the impact of an extreme perturbation event rather than a typical one. Since our trajectory results already represent an upper limit on the perturbation itself, the impact on the temperature profile computed in this case should be interpreted as a severe upper limit on the possible temperature profile perturbations, neglecting any positive feedbacks.

[17] A recent paper by *Oinas et al.* [2001] shows that different radiation schemes used in GCMs yield widely different equilibrium temperature changes produced by stratospheric water perturbations. In order to test our scheme, we compute the equilibrium temperature changes for the stratospheric water perturbations given by *Oinas et al.* [2001]. The resulting temperature change profiles compare very well with the reference profiles given in Figures 1 and 2 of *Oinas et al.* [2001]. It is commonly stated that broadband radiation models are less accurate than those with finer spectral resolutions. This is not necessarily true if the models have been derived and/or benchmarked to line-by-line computations. The water vapor thermal infrared model of *Chou* [1984] used in the *Rosenfield et al.* [1994] code was derived from and compares well with line-by-line computations.

[18] Figure 3 shows the unperturbed temperature profiles (top panels) and the accompanying perturbations (as calculated by the radiative transfer model) to the temperature profiles (bottom panels) caused by the additional water vapor from the subsonic aircraft emissions. The figure shows

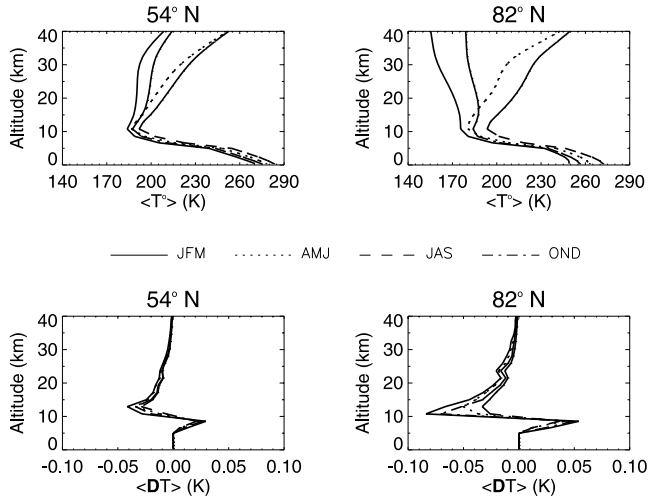

Figure 3. (top) Mean temperature profiles and (bottom) perturbations of those profiles, the latter as associated with an extreme water vapor perturbation event resulting from subsonic emissions. The left-hand column plots are associated with a perturbation profile at 54°N, while the right-hand column plots are associated with 82°N. Results were achieved using the radiative transfer model of *Rosenfield et al.* [1994].

Table 1. Radiative Forcings in W/m^2 [a]

	Winter	Summer
	Subsonic	
54°N standard	0.002	−0.001
54°N extreme	0.008	0.002
82°N standard	0.004	−0.006
82°N extreme	0.012	−0.007
	Supersonic	
2°S standard	0.111	0.111
2°S extreme	0.267	0.268
46°N standard	0.111	0.116
46°N extreme	0.199	0.207

[a]We computed the radiative forcings at the tropopause for the subsonic and supersonic water vapor perturbations predicted by the trajectory model output. The "standard" case represents the monthly mean water vapor perturbation profile, while the "extreme" case represents the monthly mean water vapor perturbation profile plus 2 standard deviations. See the text for more details.

results at each of two latitudes: 54°N and 82°N. Both of these latitudes are in the extended region of enhanced water vapor predicted in the trajectory results. We subdivide our results by season, showing 3-month averages (January/February/March, April/May/June, July/August/September, and October/November/December). Although we see large seasonal fluctuations in the temperature profiles, the absolute seasonal fluctuations in the temperature perturbations are small. At both latitudes we observe that the water vapor perturbations lead to temperature differences of not greater than 0.10 K. Our results are on the low side of the previous radiative transfer calculations of *Fortuin et al.* [1995] that indicate possible cooling at midlatitudes of 0.04–0.20 K in the summer and 0.1–0.6 K in winter.

[19] Radiative forcings in the fixed temperature mode of the radiative transfer model were calculated to determine the instantaneous forcing at the tropopause. The temperature profiles used in this calculation come from *Fleming et al.* [1988]. The resulting forcings are shown in Table 1 for January (Winter) and July (Summer) conditions. The forcings for the subsonic case are small, less than 0.012 W/m^2. Summertime negative forcings arise when the reduction of solar flux into the troposphere due to the additional water vapor is larger than the change in long wave flux caused by the presence of the additional water vapor. Note that positive values indicate increases of flux into the troposphere. In summary, the radiative forcing at the tropopause in our model shows only negligible differences from the nonperturbed case. From our results, we thus conclude (as have numerous previous studies such as those by *Ponater et al.* [1996], *Rind et al.* [1996], and *Brasseur et al.* [1998]) that the water vapor enhancements arising from subsonic aircraft have little to no impact on the temperature structure of the lower stratosphere, and thus, on the height of the local tropopause.

3.2. Supersonic Emissions

[20] Figure 2b shows the trajectory results for the equilibrium, zonal mean perturbation for June 1998 caused by the injection of water vapor from supersonic aircraft. Overlaid on the figure, as in Figure 2a, are the potential temperature surfaces (orange lines) and the tropopause (thick white line). We observe that in much of the stratosphere in both hemispheres from 10 km to 35 km, perturbations of greater than 50 ppbv occur. The strongest impact is observed in the tropics, with a peak perturbation of ~0.9 ppmv near 21 km (note: the highest peak value of 1.5 ppmv is predicted for January, not shown). A layer several kilometers thick centered around 20 km altitude shows water vapor perturbations greater than 0.2 ppmv extending from the tropics far into both hemispheres. The supersonic water vapor perturbation distribution seen in Figure 2b has a similar morphology to the superonic NO_y perturbation distribution shown in Plate 3a of *Schoeberl and Morris* [2000], again as we would expect.

[21] Our results indicate substantially different water vapor perturbations than seen in the 2-D and 3-D models reported by *Kawa et al.* [1999] and *Penner et al.* [1999]. In Figures 4–8 of *Kawa et al.* [1999] and Figure 4–6b of *Penner et al.* [1999], results from 11 models show maximum perturbations of 0.3–0.7 ppmv, somewhat smaller than the largest values we find in the trajectory model results. Most of these models show that the peak perturbation occurs between 15 and 20 km and between 30°N and 60°N, whereas our trajectory result indicates the maximum perturbation occurs around 20–23 km in the tropics.

[22] In addition, the models show perturbations of greater than 0.1 ppmv extending throughout the stratosphere, up to 60 km in altitude. In contrast, the trajectory results indicate that above 35 km, perturbations are generally below ~50 ppbv, and large perturbations (>0.5 ppmv) are confined to a layer between 10 and 25 km. Only one of these other models shows a water vapor perturbation distribution somewhat similar to that produced by our trajectory results, that being the SLIMCAT-3D Model. Even this model, however, indicates perturbation amounts of 0.3 ppmv extending from 20 to 40 km, far higher amounts of water vapor than observed in the trajectory results.

[23] In order to achieve such high water vapor mixing ratios, the water vapor source term must be greater, the loss term smaller, or both must be true for these models as compared to the trajectory model. Since the only loss term in the trajectory model is due to transport, our result suggests that less downward transport is occurring in the other models than is occurring in the trajectory model, thereby preserving higher amounts of water vapor in much of the stratosphere than seen in the trajectory results. *Schoeberl and Morris* [2000] concluded that the excessive numerical diffusion present in 3-D models and the poorly simulated stratosphere/troposphere exchange in 2-D models likely accounts for the differences in the NO_y distributions that they observed. The same conditions are also likely responsible for the differences seen here in the water vapor results.

[24] The maximum water vapor perturbation cited in the study of *Rodgers et al.* [2000] (produced using the SLIMCAT model) of ~0.4 ppmv is fairly consistent with our largest values (~0.5 ppmv as seen in Figure 2b). The water vapor perturbation results of *Kinnison et al.* [2001] as achieved with the Global Modeling Initiative (GMI) 3-D chemical transport model show very good agreement with our results. In particular, Figure 1b of *Kinnison et al.* [2001] shows the resulting water vapor perturbation caused by the presence of a fleet of high speed transports consistent with that used in our study. The morphology of the perturbation and its amount are generally consistent with our results, although the trajectory results seem to be somewhat greater in magnitude than those given by *Kinnison et al.* [2001]. Recall that unlike the GMI CTM, our model includes no loss

processes for water vapor other than transport out of the stratosphere through the tropopause. Since our goal is to determine if further, more careful study of the impact of water vapor emissions from high speed transports is warranted, the fact that our perturbation may be too large is not an issue if the impact on the radiative balance is found to be small.

[25] As with the subsonic case, we examine the radiative impact of the water vapor perturbations predicted by the trajectory model using the radiative transfer model of *Rosenfield et al.* [1994]. We calculate a monthly mean water vapor perturbation profile associated with the supersonic emissions for each month in each year of our study. Then we calculate profiles of the associated standard deviations for each month in each year of our study. Next, we construct a new and extreme set of water vapor perturbation profiles by adding to each monthly mean profile twice the associated standard deviation profile for that month and year. One of the largest resulting profiles in this new set of profiles occurs for January 1998. By using this large water vapor perturbation to initialize our radiative transfer calculations throughout the year, we are virtually assured that our calculated temperature perturbations represent a severe upper limit on the magnitude of the actual temperature perturbations. The results from our radiative transfer model for this case are identified in Figure 4 by the black lines as case A. We then examine the impact on temperatures caused by the addition of the original monthly mean water vapor perturbation profiles for January 1998. The results from our radiative transfer model for this case are identified in Figure 4 by the shaded lines as case B. This case represents a more plausible water vapor perturbation, though still larger than we would anticipate actually occurring for the same reasons we presented earlier in the subsonic case. We again subdivide our results by season, showing 3-month averages (January/February/March, April/May/June, July/August/September, and October/November/December).

[26] Figure 4 shows the unperturbed temperature profiles (top panels) and the accompanying perturbations (as calculated by the radiative transfer model) to the temperature profiles (bottom panels) caused by the additional water vapor from the supersonic aircraft emissions. The figure shows results at each of two latitudes: 2°S and 46°N. Both of these latitudes are in the extended region of perturbed water vapor predicted in the trajectory results, and the former of the two is collocated with the maximum perturbation observed in the tropics. We subdivide our results by season, showing 3-month averages (January/February/March, April/May/June, July/August/September, and October/November/December).

[27] Our results suggest a more substantial impact on temperatures from the supersonic emissions than is seen in the subsonic case. Temperature changes with magnitudes of up to 1.8 K are observed in case A just above the tropopause at 2°S, while changes with magnitudes of up to 0.55 K are found at 46°N. Similar results, though of smaller magnitude, are observed for case B, with peak cooling of less than 1 K at 2°S and less than 0.5 K at 46°N. At both latitudes, cooling occurs throughout the stratosphere above ~15 km, and a thin layer of warming occurs near the tropopause. Just above the warmed layer is the layer of maximum cooling. These results are consistent with those reported by *Brasseur et al.* [1998] for a GCM study that included doubling of water vapor in the stratosphere from supersonic emissions.

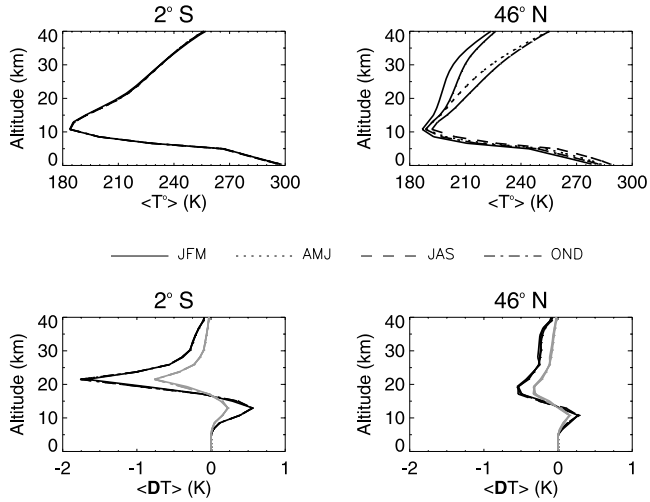

Figure 4. As in Figure 3, but for supersonic perturbations. In this case, the left-hand plots are associated with 2°S, while the right-hand column plots are associated with 46°N. The black lines (case A) are associated with the mean-plus-2 standard deviation perturbation, while the shaded lines (case B) are associated with the mean perturbation.

[28] If the actual temperature profile is slightly different than the one we used, such a vertical structure in the temperature perturbation could blur the boundary between the troposphere and the stratosphere and potentially increase tropopause height in the tropics and midlatitudes. A warmer tropopause in the tropics might lead to increases in the flux of water vapor into the stratosphere and the subsequent formation of polar stratospheric clouds. Our radiatively determined profiles, however, do not indicate a change in tropopause height.

[29] The radiative transfer calculations indicate that changes in radiative forcing at the tropopause are an order of magnitude greater for the supersonic than for the subsonic case, as can be seen in the data in Table 1. In this table, the "standard" case represents our case B, while the "extreme" case represents our case A. Again, we define our radiative forcing so that positive values indicate fluxes into the troposphere. It is hard to compare our forcings with those previously published by *Fortuin et al.* [1995] in their Table 1 since their initialization conditions for the water vapor perturbation are quite different from ours. Whereas we use profiles predicted from the trajectory calculations, *Fortuin et al.* [1995] initialize a water vapor perturbation in a layer of constant mixing ratio from the tropopause to the top of the flight corridor. Since the tropopause is much higher in summertime, they have much less total water vapor in the stratosphere during summer than winter. Consequently, they find substantially lower forcings in summer than winter. Since the trajectory approach allows for the accumulation of water vapor in the stratosphere throughout the year, we believe our results (our Table 1) represent a more realistic scenario. As a result of our conservative approach, we do not see substantially different forcings between summer and winter. Nevetheless, our midlatitude wintertime forcings are of the same order of magnitude as those of *Fortuin et al.* [1995].

[30] As in the subsonic case, our results should be viewed as an upper limit on the possible consequences of supersonic exhaust on the temperature structure of the lower stratosphere rather than a likely result.

4. Summary and Conclusions

[31] We have presented in this work a dynamical simulation that represents an upper limit to the perturbation in stratospheric water vapor and temperatures that can result from emissions of subsonic aircraft and a proposed fleet of supersonic transports. Our results show that in the subsonic case, the largest perturbations are confined to a region near the tropopause in the Northern Hemisphere, between 30°N and 90°N. Maximum values for the subsonic pertubation of <150 ppbv are observed in February. Radiative transfer calculations indicate that the subsonic aircraft have little impact on the temperature structure of the lower stratosphere.

[32] For the supersonic case, the largest water vapor perturbations of ~1.5 ppmv occur in the tropics near 22 km in January. While such maximum values are somewhat larger than those reported by *Kawa et al.* [1999], the spatial extent of values of >0.2 ppmv found in the results of other models greatly exceeds that indicated in the trajectory model results. In particular, the trajectory model shows perturbations not exceeding 50 ppbv above 35 km where many 2-D and 3-D models show values of as high as 0.3 ppmv. As suggested by *Schoeberl and Morris* [2000], the difference is likely due to excessive vertical diffusion in 3-D models and sluggish stratosphere/troposphere exchange in the 2-D models.

[33] Radiative transfer calculations using water vapor perturbations from our supersonic case indicate changes with magnitudes of up to 1.8 K in the temperature profile in the most extreme cases. Most of the stratosphere experiences some cooling, while a thin layer near the tropopause warms. Such changes may warrant a further analysis beyond the scope of this study. A warmer tropopause would permit a higher flux of water vapor to enter the stratosphere in the tropics, resulting in a positive feedback that could result in more PSCs and subvisible cirrus clouds. The former effect may result in more significant losses in polar ozone during the spring season in the Northern Hemisphere, while the latter effect could further impact the temperature structure in the region near the tropopause.

[34] In both the subsonic and supersonic cases, our results should be viewed as an upper limit to the possible changes in the water vapor and temperature structure of the lower stratosphere as our model includes no loss mechanisms for the water vapor other than transport to and subsequent rainout in the troposphere. Furthermore, our radiative calculations are based upon water vapor profiles two standard deviations larger than some of the largest perturbations observed in our study.

[35] **Acknowledgments.** This research was funded by NASA's Atmospheric Effects of Aviation Program and the EOS Interdisciplinary Science Program. We would like to thank the reviewers for their helpful comments for improving our manuscript.

References

Bakan, S., M. Betancor, V. Gayler, and H. Grassl, Contrail frequency over Europe from NOAA-satellite images, *Ann. Geophys.*, *12*, 962–968, 1994.

Baughcum, S. L., et al., Scheduled civil aircraft emission inventories projected for 2015: Database development and analysis, NASA CR-1998-207638, NASA Goddard Space Flight Cent., Greenbelt, Md., 1998.

Brasseur, G. P., R. A. Cos, D. Hauglustaine, I. Isaksen, J. Lelieveld, D. H. Lister, R. Sausen, U. Schumann, A. Wahner, and P. Wiesen, European scientific assessment of the atmospheric effects of aircraft emissions, *Atmos. Environ.*, *32*, 2329–2418, 1998.

Chou, M.-D., Broadband water vapor transmission functions for atmospheric IR flux computations, *J. Atmos. Sci.*, *41*, 1775–1778, 1984.

Danilin, M. Y., et al., Aviation fuel tracer simulation: Model intercomparisons and implications, *Geophys. Res. Lett.*, *25*, 3947–3950, 1998.

Fleming, E. L., S. Chandra, M. R. Schoeberl, and J. J. Barnett, Monthly mean global climatology of temperature, wind, geopotential height, and pressure for 0–120 km, NASA Tech. Memo., 100697, 1988.

Fortuin, J. P. F., R. van Dorland, W. M. F. Wauben, and H. Kelder, Greenhouse effects of aircraft emissions as calculated by a radiative transfer model, *Ann. Geophys.*, *13*, 413–418, 1995.

Gettelman, A., The evolution of aircraft emissions in the stratosphere, *Geophys. Res. Lett.*, *25*, 2129–2132, 1998.

Gettelman, A., and S. Baughcum, Direct deposition of subsonic aircraft emissions into the stratosphere, *J. Geophys. Res.*, *104*, 8317–8327, 1999.

Kawa, S. R., et al., Assessment of the effects of high-speed aircraft in the atratosphere, NASA/TP-1999-209237, NASA Goddard Space Flight Cent., Greenbelt, Md., 1999.

Kinnison, D. E., et al., The Global Modeling Initiative assessment model: Application to high-speed civil transport perturbation, *J. Geophys. Res.*, *106*, 1693–1711, 2001.

Marquart, S., R. Sausen, M. Ponater, and V. Grewe, Estimate of the climate impact of cryoplanes, *Aerosp. Sci. Technol.*, *5*, 73–84, 2001.

Nevison, C. D., S. Solomon, and R. S. Gao, Buffering interactions in the modeled response of stratospheric O_3 to increased NO_x and HO_x, *J. Geophys. Res.*, *104*, 3741–3754, 1999.

Oinas, V., et al., Radiative cooling by stratospheric water vapor: Big differences in GCM results, *Geophys. Res. Lett.*, *28*, 2791–2794, 2001.

Penner, J. E., D. H. Lister, D. J. Griggs, D. J. Dokken, and M. McFarland (Eds.), Aviation and the Global Atmosphere, Cambridge Univ. Press, New York, 1999.

Ponater, M., S. Brinkop, R. Sausen, and U. Schumann, Simulating the global atmospheric response to aircraft water vapour emissions and contrails: A first approach using a GCM, *Ann. Geophys.*, *14*, 941–960, 1996.

Rind, D., P. Lonergan, and K. Shah, Climatic effect of water vapor release in the upper troposphere, *J. Geophys. Res.*, *101*, 29,395–29,405, 1996.

Rind, D., P. Lonergan, and K. Shah, Modeled impact of cirrus cloud increases along aircraft flight paths, *J. Geophys. Res.*, *105*, 19,927–19,940, 2000.

Rodgers, H. L., M. P. Chipperfield, S. Bekki, and J. A. Pyle, The effects of future supersonic aircraft on stratospheric chemistry modeled with varying meteorology, *J. Geophys. Res.*, *105*, 29,359–29,367, 2000.

Rosenfield, J. E., The impact of subvisible cirrus clouds near the tropopause on stratospheric water vapor, *Geophys. Res. Lett.*, *25*, 1883–1886, 1998.

Rosenfield, J. E., P. A. Newman, and M. R. Schoeberl, Computations of diabatic descent in the stratospheric polar vortex, *J. Geophys. Res.*, *99*, 16,677–16,689, 1994.

Schoeberl, M. R., and G. A. Morris, A Lagrangian simulation of supersonic and subsonic aircraft exhaust emissions, *J. Geophys. Res.*, *105*, 11,833–11,839, 2000.

Schoeberl, M. R., and L. Sparling, Trajectory modeling, in Diagnostic Tools in Atmospheric Physics, vol. 124, Proceedings of the International School of Physics, Enrico Fermi, edited by G. Fiocco and G. Visconti, pp. 289–306, IOS Press, Amsterdam, 1995.

Schoeberl, M. R., C. Jackman, and J. Rosenfield, A Lagrangian estimate of aircraft effluent lifetime, *J. Geophys. Res.*, *103*, 10,817–10,825, 1998.

Swinbank, R., and A. O'Niell, A stratosphere-troposphere data assimilation system, *Mon. Weather Rev.*, *122*, 686–702, 1994.

Weaver, C. J., A. R. Douglass, and D. B. Considine, A 5-year simulation of supersonic aircraft emission transport using a three-dimensional model, *J. Geophys. Res.*, *101*, 20,975–20,984, 1996.

Wennberg, P. O., et al., Removal of stratospheric O_3 by radicals: In situ measurements of OH, HO_2, NO, NO_2, ClO, and BrO, *Science*, *266*, 398–404, 1994.

C. H. Jackman and M. R. Schoeberl, Mail Code 916, NASA Goddard Space Flight Center, Greenbelt, MD 20771, USA.

G. A. Morris, Department of Physics and Astronomy, Rice University, 6100 Main Street, MS-61, Houston, TX 77251-1892, USA. (gmorris@rice.edu)

J. E. Rosenfield, GEST Center, 3.002 South Campus, University of Maryland Baltimore County, 1000 Hilltop Circle, Baltimore, MD 21250, USA.